

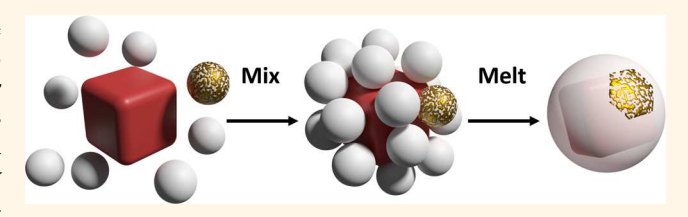
Mix-and-Melt Colloidal Engineering

Theodore Hueckel and Stefano Sacanna*®

Molecular Design Institute, Department of Chemistry, New York University, 29 Washington Place, New York, New York 10003, United States

Supporting Information

ABSTRACT: Increasing significance is being placed on the synthesis of smart colloidal particles, since the route to various meta-materials has been outlined through their bottom-up self-assembly. Unfortunately, making particles with well-defined shape and surface chemistry often requires considerable effort and time, and as such, they are available only in restrictive yields. Here we report a synthetic methodology, which we refer to as mix-and-melt



reactions (MMR), that allows for rapid prototyping and mass production of anisotropic core-shell colloids. MMR take advantage of the synergistic properties between common colloidal suspensions by aggregating then reconfiguring polystyrene shell particles onto core particle substrates. By systematically exchanging cores and shells, the resultant coreshell particle's properties are manipulated in a modular fashion. The influence of the constituent particles' size ratio is extensively explored, which is shown to tune shell thickness, change the aspect ratio of shells on anisotropic cores, and access specific shapes such as tetrahedra. Beyond particle shape, mixed shell systems are utilized to create regular surface patches. Surface Evolver simulations are used to demonstrate how randomly packed clusters melt into regular shapes via a shell compartmentalization mechanism.

KEYWORDS: anisotropic colloids, self-assembly, shape-changing, core—shell, patchy particles

vital goal of chemistry is discovering ways to gain functionality from simple starting materials. Scientists today are working to create matter that contains within it intricate microscale features to unlock useful material properties, such as manipulating sound, heat, and light. 1-7 Many advances have been made to directly write this level of detail via top-down approaches such as multiphoton lithography, which are currently capable of generating threedimensional structures of arbitrary complexity with nanoscopic resolution;⁸⁻¹¹ however bulk-scale production remains an elusive achievement. To meet this challenge, systems of discrete colloidal units have been envisioned that, through programmed interactions, can self-assemble to achieve a desired structure in a bottom-up fashion. 12-16 Today, colloidal engineering has become an enormous research effort, with a major focus placed on creating increasingly intelligent particles scalably, such that macroscopic materials can be assembled. Currently, there are many synthetic routes for chemists to take to imbue functionality into a colloidal suspension. Notably, heterogeneous nucleation is a major tool that is used to make numerous products, including core-shell particles of all shapes and sizes, ¹⁷⁻²³ particles with specific and regular geometries, ^{24,25} and even particles with distinguished surface patches. 26-29 Despite the broad utility of growing material directly on a substrate in a seeded-growth fashion, any approach relying on inherently chaotic nucleation and growth chemistry can suffer from irregularity unless strict protocols are adhered to. Furthermore, precious research time must often be committed to readapt old procedures to the next system.

Mix-and-melt reactions (MMR) offer a simple strategy for particle synthesis that circumvents traditional chemical reactions by taking advantage of the natural surface charge of common suspensions in conjunction with the shaping force of surface tension. Instead of growing shell material on a substrate, shell particles are self-assembled around a core particle, which are then fused together in regular ways by plasticization. Through MMR, many of the colloidal morphologies described above can be synthesized, as well as some that were previously unobtainable. The modular nature of this technique allows for the rapid prototyping of complex particles by exchanging different core and shell suspensions to manipulate the products' shape and surface chemistry. MMR achieve higher functionality from simple starting materials and present a fascinating mechanism for order to arise from a chaotic system, whose assembly principles can be explored both in vitro and in silico.

RESULTS AND DISCUSSIONS

Mix-and-Melt Reactions. MMR can be summarized in two basic steps: core-shell clusters are first formed via heteroaggregation by mixing oppositely charged suspensions; the clusters' shells are then processed into more regular

Received: January 19, 2018 Accepted: April 2, 2018 Published: April 2, 2018

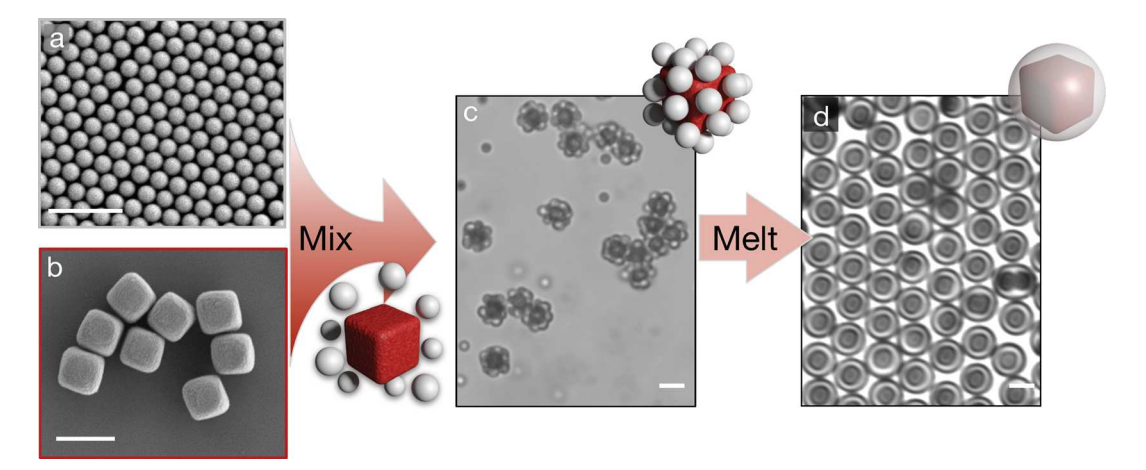


Figure 1. Mix-and-melt fundamentals. (a) Monodispersed sulfonated polystyrene shell particles. (b) Pseudocubic hematite core particles. (c) Clusters formed immediately after core and shell mixing. (d) Spherical core—shell particles formed after melting the polystyrene shells with a THF treatment. All scale bars are 2 μ m.

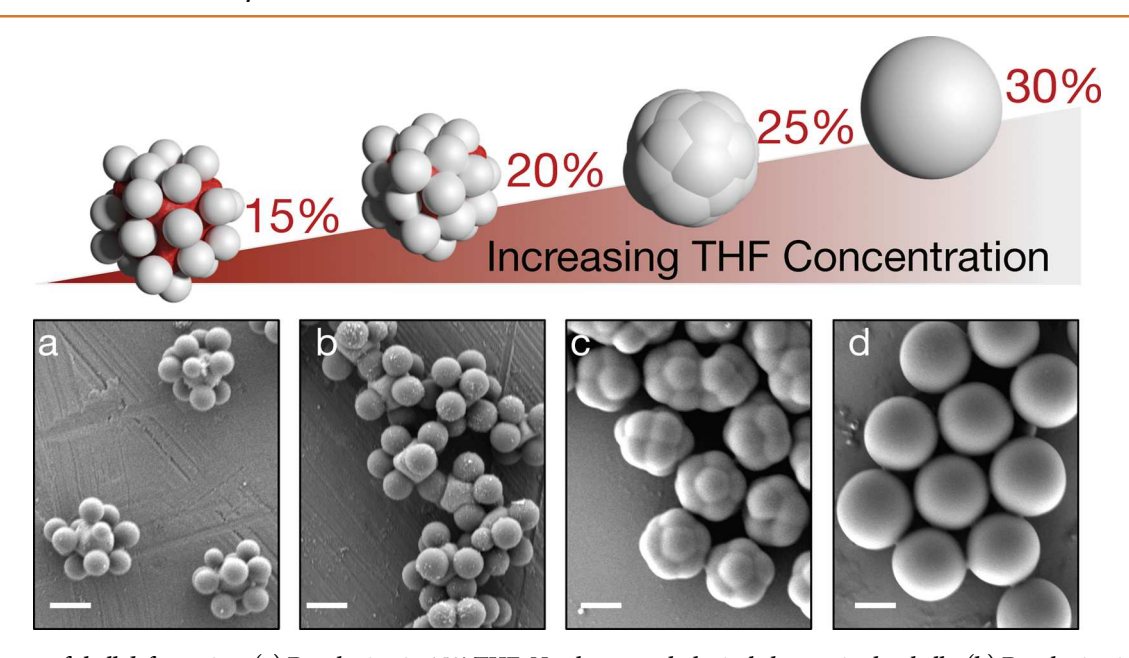


Figure 2. Stages of shell deformation. (a) Developing in 15% THF. No clear morphological changes in the shells. (b) Developing in 20% THF. The shells begin to deform and wet their cores. (c) Developing in 25% THF. The shells take on a cellular configuration, fully wetting the cores, while pressing against one another to form new interfaces. (d) Developing in 30% THF. The shells have become fully spherical, and seams between shells have vanished. All scale bars are 1 μ m.

morphologies by melting them *via* the addition of a plasticizer (see Figure 1). In all cases the shell particles are made of polystyrene, which are ideal because they can be made in a monodisperse fashion, with positive or negative surface charge, in a wide range of sizes, and on the gram scale. Since the surface charge on polystyrene can be varied, there are many core materials suitable to promote heteroaggregation. In Figure 1, cubic hematite particles are used as a model core due to their high density and optical contrast with polystyrene.

During coordination, the desired core—shell cluster product can be ruined if shells bind multiple cores together to form bridged structures. Hematite's characteristic red color makes it easy to distinguish clusters with a single core from clusters that are bridged together and contain multiple cores; yield determinations can then be used to tune the reaction conditions, whereby utilizing a larger number of shells per core minimizes the presence of bridged structures (see Figure

S1 in the Supporting Information). For clusters that do not use hematite cores, fluorescence can also be helpful to determine yields. Since a large excess of shell particles must be used during coordination to mitigate bridging, hematite's high density helps to purify the clusters from the unreacted shells. After coordination, the pink cluster product can be seen rapidly sedimenting from the remaining white polystyrene spheres, which can then be extracted and recycled.

Although heteroaggregation leads to irregular spacing between the individual shells in clusters, during the melt stage those shells become highly uniform. Plasticizer, water-soluble tetrahydrofuran (THF), is added directly to the cluster reaction mixture for 20 seconds, which allows the polystyrene to flow, reconfigure, and fuse together. The core—shell particles formed gain some notable characteristics; for example they are monodispersed (see Figure S2 in the Supporting Information), spherical and their cores are centered (Figure 1d).

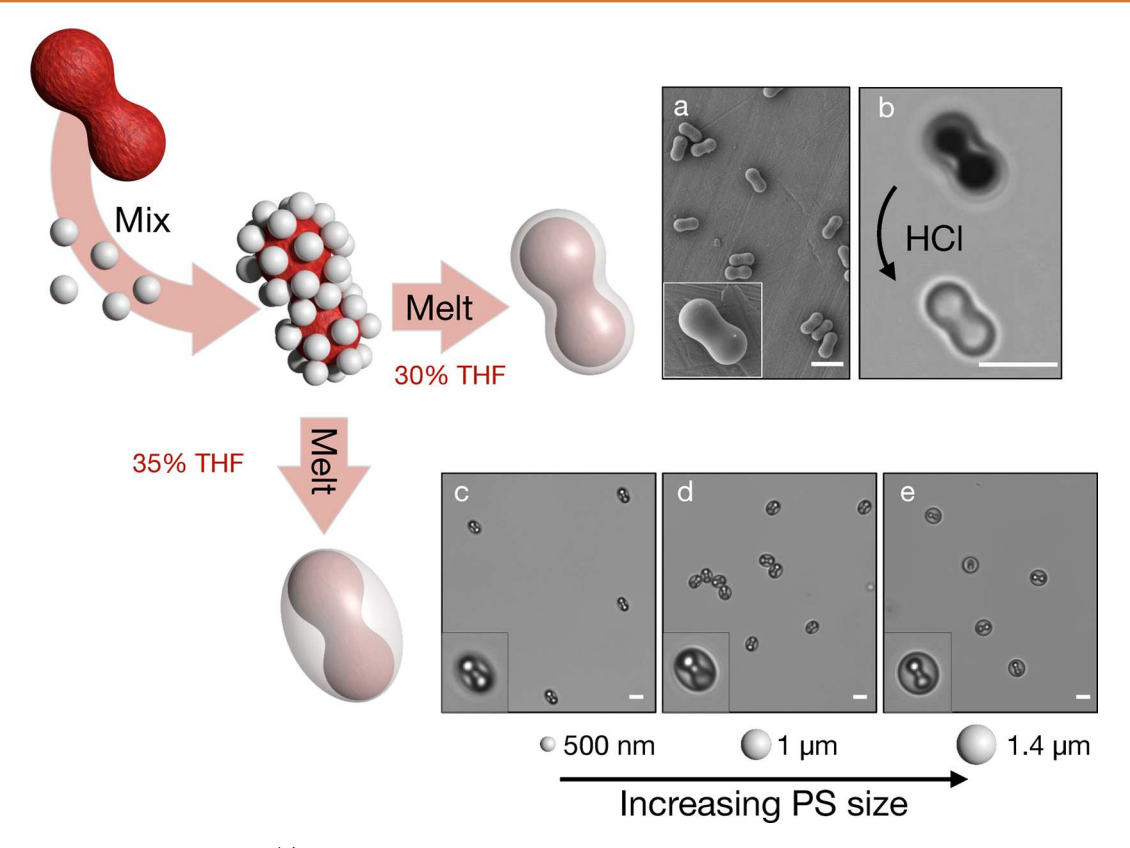


Figure 3. Influence of core anisotropy. (a) SEM image of seamless peanut-shaped shells formed with moderate concentrations of THF. (b) Before and after HCl treatment resulting in selective core dissolution, yielding a hollow peanut replica. (c-e) Ellipsoids with tunable aspect ratios formed with higher concentrations of THF. Thin ellipsoids, thick ellipsoids, and spheres formed from 500 nm, 1 μ m, and 1.4 μ m polystyrene spheres, respectively, on a 3 μ m long hematite peanut core. All scale bars are 3 μ m.

Deformation ends when the reaction is quenched with water, which solidifies the shells.

Product uniformity is explained by the shells collective behavior during plasticization. In certain conditions, such as high temperatures or in organic solvent, polystyrene softens and its shape becomes heavily influenced by surface tension. Various shapes of polystyrene particles in these conditions will simply minimize their own surface area by taking on a spherical shape.³⁰ Particles in larger assemblies, however, consider the energetics of the whole and consequently adopt a variety of morphologies to minimize surface energy. ^{24,31-33} Despite being in a liquid state, individual shell particles retain a distinct identity during deformation, which can be seen in detail when developing the clusters in varying concentrations of THF (see Figure 2). By forming interfaces with one another during deformation, instead of coalescing, the polystyrene shells become a contiguous whole made of compartments, which evolves into regular geometric morphologies.

Four distinct states of deformation exist between the initial cluster and its final spherical form. Below a developing concentration of 15% THF there is no visible change in shells; however these clusters are more robust, since they can be sonicated and dried out without the shells disassembling from the cores (Figure 2a). At 20% THF the first changes in the shape of the shells become apparent, whereby the shells begin to wet their cores (Figure 2b). Increasing the concentration to 25% leads to a state where regular geometric patterns begin to arise. Here, the shells have fully engulfed the cores and are pressing against one another to form a cellular architecture, where the compartments present as various polygons (Figure

2c). Finally, at concentrations of 30% and up the seams that previously showed a clear demarcation between shells fade and the final spherical core—shell product is reached (Figure 2d). This general deformation behavior is observed for differently sized shells in a variety of cluster types (see Figure S3 and Figure S4 in the Supporting Information).

The two stages of MMR are not volume restrictive, and as such, reactions carried out with a few microliters of particles behave similarly to those that use hundreds of milliliters. This makes it possible to prepare many small batches of particles to survey a large variety of conditions, while being able to faithfully scale up successful small batches. In comparison, seeded growth syntheses, which often require a steady monomer drip or constant stirring, often cannot be carried out on minute volumes of cores, and scaling up means reoptimizing the reaction conditions to account for variables such as shear and drip rate. Currently the only shell material successfully utilized is polystyrene, which can be modified in a number of ways, but is ultimately a synthetic limitation. Other polymeric materials such as poly(methyl methacrylate) (PMMA) hold potential to serve as shells for MMR, since they have previously been shown to display compartmentalization when melted.³¹ Expanding the list of proper shell materials will require searching for particles that can be controllably melted and resolidified via a glass transition.

Core Shape Influence. Anisotropically shaped cores can influence how the shells develop, further expanding the list of morphologies made accessible *via* MMR. Peanut-shaped hematite particles can be used as cores, for example, and clusters are produced, processed, and purified in the same

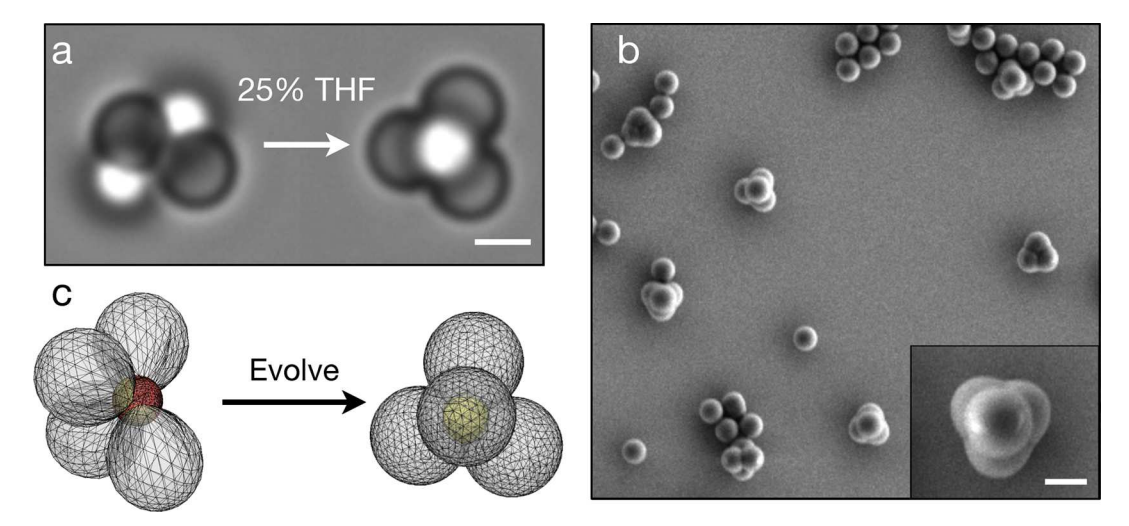


Figure 4. Cellular symmetry. (a) Two clusters, before and after treatment with THF. The initial skewed configuration becomes tetrahedrally symmetric with a treatment of 25% THF. (b) SEM image of tetrahedral clusters treated with 25% THF. Most excess shells were removed by isopycnic centrifugation. (c) Results of simulations run on Surface Evolver. Initial construct includes four asymmetrically coordinated shells (white) on a core particle (red). Evolution of the starting construct under the influence of surface tension results in the shells reconfiguring into a tetrahedral symmetry cluster. All scale bars are $1 \mu m$.

fashion as cubic-cored clusters. The development of their shells, however, reveals a different dynamic when reaching the seamless state, yielding two different morphologies, a peanut and an ellipsoid (Figure 3). From this we can see the competition between shells as individuals and shells as a collective. While the ellipsoidal shell minimizes the overall surface area, more radical deformations must occur in the individual shell particles to achieve this state, particularly around the belt and at the tip of the peanut core. A peanut-shaped shell, alternatively, accepts a higher surface area while keeping the relative deformation between individual shells more uniform, demonstrated by the peanut shells constant thickness.

Deformation into a peanut-shaped shell reveals the capability of MMR to replicate the shape of their underlying cores (Figure 3a). Through moderate deformation conditions, followed by the selective etching of the underlying core, a hollow polystyrene peanut is produced (Figure 3b). Previously, replication had only been demonstrated by solid materials such as silica and titania, 18,19 although polystyrene replicas offer advantages such as low density for assembling larger three-dimensional structures.

Ellipsoidal shells are prepared by increasing the developing THF concentration to 35%, which allows surface tension to dominate as the polystyrene behaves as fully liquid. Although spheres have a lower surface area than ellipsoids, there may not be a large enough volume of shell material to form a sphere around the core. By selecting differently sized shell particles during coordination, however, the volume of shell material can be tuned to affect the resulting ellipsoid's shape. A clear trend emerges, whereby the ellipsoid's thickness increases as shell particle size increases (Figure 3c-e). Through shell size selection the aspect ratio of the ellipsoidal shell can change drastically from skinny ellipsoids to fully spherical shells that arise from larger shell particles. A strength of MMR is the flexibility in starting materials that can be used, and anisotropic cores make a dynamic range of morphologies accessible, from ellipsoids with tunable aspect ratios to peanut-shaped replicas.

Cellular Shell Symmetry. Despite the chaotic nature of coordination, the products of MMR spontaneously gain symmetry during the melt phase. This phenomenon is

attributed to two concurrent events, namely, the liquefaction and compartmentalization of shell particles. Reconfiguration is necessary to achieve ordered structures, and the pliability of shells under the influence of plasticizer allows surface tension to do that work, while the cellular network of shells serves as a guide for regular geometries to emerge, such as the polygonal faces presented in Figure 2c. In addition to those two-dimensional features, specific three-dimensional structures can also be targeted *via* MMR. Here, we consider how the coordination number of a cluster can relate to a specific symmetric minimum surface energy structure and how evolution to that state may happen in spite of the cluster's originally random shell placement.

Targeting a specific geometry requires the production of clusters with equivalent coordination numbers, which can be difficult to achieve since there are many ways shell particles can park during coordination, leading to a broad product distribution. It has previously been shown, however, that tetramers can be coordinated in quantitative yields because at the appropriate core:shell size ratio none of the trimer isomorphs prohibit tetramer coordination and none of the tetramer isomorphs allow higher coordination.³⁴ Fortunately, tetrahedral clusters are in high demand, 35-37 although clusters produced by heteroaggregation are not suitable for further assembly due to their asymmetry. Treatment of an asymmetric cluster with 25% THF, however, allows the shells to reconfigure into a symmetric tetrahedron (Figure 4a). Clusters here are produced with silica cores and purified via isopycnic centrifugation, which creams unreacted shells while sedimenting the more dense cluster product (Figure 4b). Through MMR, a significantly larger scale of tetrahedral clusters may become accessible than the current state of the art allows by circumventing the density gradient centrifugation required for clusters produced by emulsion evaporation. There is only a slight difference in density between clusters and excess shells, which grants efficient purification of the dense core product. Tetrahedral clusters with low-density cores or higher density shells, utilizing PMMA for instance, may not be separable with isopycnic centrifugation and may require density gradient centrifugation.

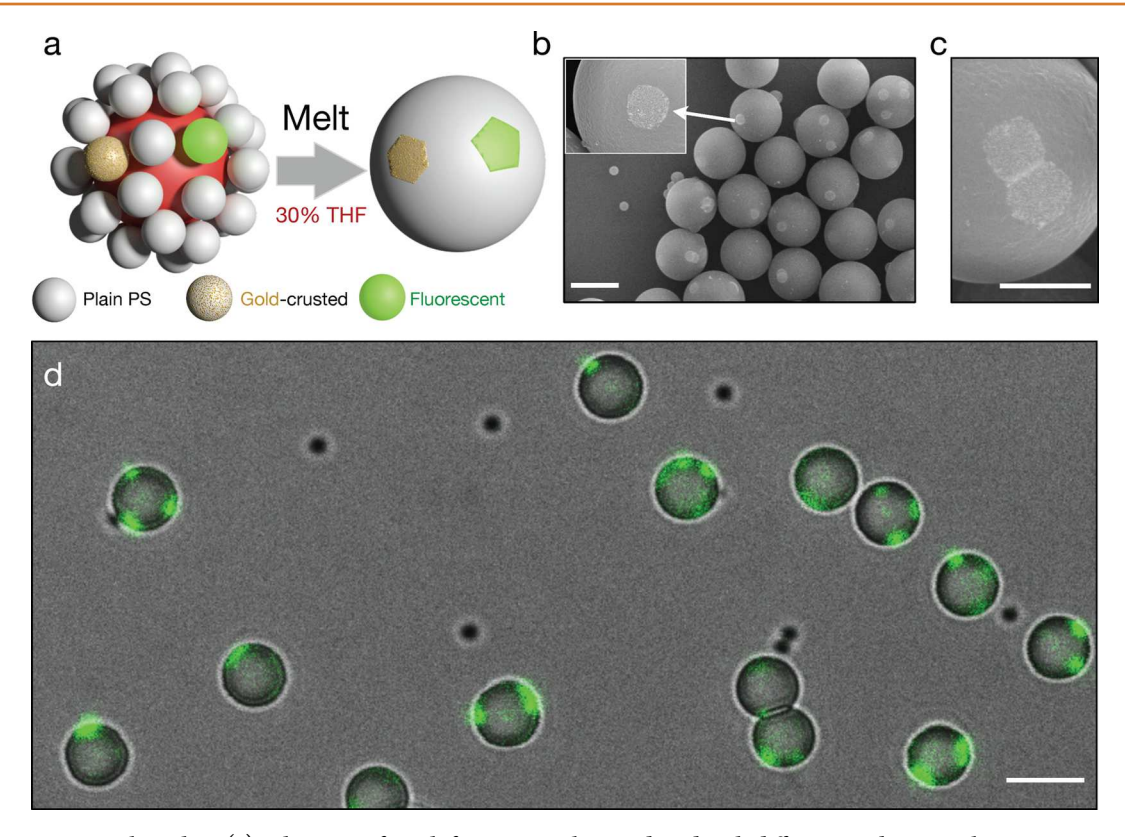


Figure 5. Compartmental patches. (a) Schematic of patch formation. Clusters doped with different marker particles are processed in THF to form distinct surface patches. Marker particles can widely vary in functionality, from nanoparticle coatings to containing cross-linked fluorescent groups. (b-c) SEM images of gold patch particles under low and high magnification. Random numbers of gold patches are randomly positioned on the surface of the particles after the melt stage. High magnification reveals that patches can have polygonal morphologies, determined by the number of nearest neighbors the marker particle has after coordination. Scale bars are 1 μ m. (d) Confocal microscopy image of fluorescent patchy particles. Localized fluorescent signal demonstrates distinct compartmental patches. Scale bar 3 μ m.

To aid in understanding how symmetry can be generated in plasticized clusters, Surface Evolver³⁸ simulations are utilized, which can apply the same constraints present in the physical system, i.e., distinct shell particles enveloping a solid core under the influence of surface tension. In the simulation an asymmetric cluster, with three distinct surfaces defined by red, yellow, and white interfaces, is evolved to allow the shells to wet, spread, and reconfigure, ultimately yielding a symmetric tetrahedral cluster (Figure 4c). The low surface tension core/ shell interface represented by the yellow color spreads, making the shells wet the core and forcing the red core interface to shrink. Surface Evolver proves to be a powerful predictive tool, since the cellular shell symmetry empirically observed on a spherical core can be faithfully reproduced in silico. Furthermore, the core constraint formula can be varied to see what conformation a shell might take on other core shapes to help predict morphologies and deformation behaviors (see Figure S5 in the Supporting Information).

Polygonal Surface Patches. Compartmentalization also allows shell particles to retain distinct chemical identities during plasticization, which can lead to more complex surface functionality. Clusters are doped with distinct marker shells that develop into easily distinguishable surface patches (Figure 5a). Two types of marker particles are investigated to probe the various aspects of patch formation: gold crusted and fluorescently labeled polystyrene shells, demonstrating limited diffusion of species on the surface of and in the bulk of shells, respectively.

Clusters are coordinated with 10% gold marker shells (Figure 5b), then deformed to a seamless state and dried on a silicon wafer. Distinct but randomly placed gold patches are visible *via* SEM with sharp contrast between patch and non-patch areas. Close inspection reveals that patches can retain the polyhedral morphologies demonstrated at the cellular stage of deformation (Figure 5c), showing that there is an underlying compartmental structure to the shells even though there are no clear seams between them. These seams can, however, be seen clearly in deformed aggregates of pure gold marker shells (see Figure S6 in the Supporting Information). Gold patches, aside from serving as good electron beam contrast, can undergo postmodification with a range of thiols to gain functionality. Furthermore, a variety of nanoparticles can be used to decorate marker shells, making patch synthesis more flexible.

Fluorophores can be cross-linked directly into the polystyrene during its synthesis to show how shell material diffuses during plasticization. Figure 5d shows a composite fluorescence and bright field image acquired *via* scanning confocal microscopy, where the fluorescent shell material stays localized, while the surrounding polystyrene shell remains nonfluorescent. Increases in the developing THF concentration can lead to compartmental breakdown and a more diffuse fluorescent signal (see Figure S7 in the Supporting Information). Polystyrene can be synthesized with various cross-linkable groups to later facilitate functionalization, 41 so the isolated fluorescent signals suggest that postmodification can occur distinctly on the patches.

Although patches are random in number and placement, they can be synthesized in a modular fashion and appear in interesting morphologies. A variety of polygonal patches, for example, have been observed (Figure 5c), and the concept of patch shape is not often explored because most synthetic procedures yield circular patches. More advanced coordination techniques could be used to program a marker particle to have specific polygonal shapes that bind strongest when patches are in register, leading to orientation specific binding schemes; a feat that circular patches cannot realize.

CONCLUSIONS

Taken together, these results demonstrate that the holistic synthetic approach offered by MMR has great potential for colloidal engineering. The general and modular nature of MMR open a world of possibilities through a variety of core—shell combinations coming together under different conditions. Many advancements can be made from this point, although most importantly, techniques should be perfected to predesign a variety of more uniform clusters, since controlling the placement and composition of shells will allow MMR to form complex shapes and surface patterns.

METHODS

Mixing Oppositely Charged Particles to Form Clusters. Clusters are assembled from positive or negative polystyrene sphere shells and various oppositely charged core materials including silica, hematite, and solid 3-(trimethoxysilyl)propyl methacrylate (TPM) particles *via* a simple heteroaggregation process.

Cores. Various monodispersed hematite suspensions are produced via the gel—sol method adapted from Sugimoto. Silica is prepared using the Stöber method. Solid TPM particles are prepared by the hydrolysis and condensation reaction of TPM (\geq 98% from Sigma-Aldrich). A 40 μ L amount of NH3 (28% wt) is added to 160 mL of deionized water, followed by the addition of 300 μ L of TPM monomer. This mixture is kept under mild magnetic stirring for 1 h to allow the oil droplets to nucleate and grow to a final size of approximately 800 nm. By changing the ratio of ammonia and oil precursor, the droplet size can be tuned from 400 nm to over 1 μ m. The emulsions were fluorescently labeled using rhodamine-B isothiocyanate to allow for fluorescence microscopy. The emulsions are solidified by the addition of 50 mg of azobis(isobutyronitrile) and heating the suspension to 80 °C for 2 h.

Polystyrene Shells. Polystyrene particles of approximately 600 nm in diameter are prepared by surfactant-free emulsion polymerization using 2,2-azobis(2-methylpropionamidine) dihydrochloride (AIBA) or potassium persulfate (KPS) as a radical initiator for positive and negative shells, respectively. A 50 mL amount of styrene monomer (≥99% from Sigma-Aldrich) is added to a 1 L three-neck round-bottom flask containing 500 mL of deionized water. The mixture is set under a nitrogen atmosphere and emulsified by mechanically stirring at 330 rpm. A 0.5 g amount of either initiator is added, and the temperature is raised to 60 °C. After 16 h the mixture is brought to room temperature, and the particles are washed in deionized water *via* multiple sedimentation and resuspension cycles. Larger particles (>600 nm) are obtained by seeded growth.

Mixing. Clusters are assembled by the rapid addition of a dilute core suspension to an equal volume of concentrated shell suspension, typically 0.8 wt % polystyrene, while aggitating by hand. The core concentration is variable with the coordination number of the clusters, where a core:shell number ratio of 1:100 is appropriate for tetramers, while 1:3000 is necessary for clusters with a coordination number of 10. The coordination is done within seconds, although clusters are kept in suspension with a Waverly S2L-Pro linear shaker.

Melting Polystyrene Particles into Uniform Shells. The liquefaction of polystyrene is initiated by introducing a water-soluble plasticizer (THF) to the cluster suspension. Depending on the desired

level of deformation, the developing concentration of THF may vary; in each case a 40% v/v THF stock is used to reach the developing concentrations reported. After 20 s of deformation, the suspension is diluted by a factor of 4 with deionized water to quench the reaction. Suspensions are subsequently washed in deionized water *via* multiple centrifugation and resuspension cycles.

Core Dissolution. Hematite will etch over 12 h in 6 M HCl to yield hollow polystyrene replicas. The suspension can be stabilized during the etching procedure with Pluronic F-108 to prevent aggregation.

Gold Crust. Gold crusts are formed by following previous work, ⁴⁵ replacing silica with positively charged polystyrene.

Dynamic Light Scattering. Dynamic light scattering experiments were carried out with a Malvern Zetasizer Nano ZS.

Simulations. We use Surface Evolver version 2.70 to simulate the transformation of asymmetric tetrameric clusters into symmetric tetrahedral clusters. A script file defines an initial surface, here an asymmetric cluster of four bodies connected to a central core constraint (see Supplementary Surface Evolver script). The surface is converted to a tessellation of triangles, which, when evolved, adopt a minimal energy conformation *via* a gradient descent method. The triangular mesh can also undergo various operations, such as subdivision to refine the structure, as well as the deletion of smaller triangles for vanishing surfaces.

To simulate mix-and-melt reactions, we consider a cluster comprising four liquid polystyrene shells assembled around a solid core particle. The core remains solid through a constraint formula defining a sphere, although the core constraint formula can be modified to represent a variety of core shapes. Interfacial tensions are defined for the following interfaces: shell/water, core/water, and core/shell, which are set *ab initio*, but can be modified during evolution to simulate changing conditions.

A typical simulation begins with the following conditions: (i) shell/water interface set to 50 mN m⁻¹ and core/shell interface set to 1 mN m⁻¹, chosen to match values previously used;³² (ii) the core/water interface is set to 85 mN m⁻¹; (iii) the core-to-shell size ratio, set by the core constraint formula and final shell size, is set to 1:2, a ratio typically used to make tetrahedra. A typical evolution protocol (see Figure S8 in the Supporting Information) comprises mesh refinement, evolution iterations, and weeding out of vanishingly small triangles. For the shells to wet the core, it is necessary to weed out vanishingly small triangles. In Figure 4c the initial construct is first evolved with a high shell/water tension of 100 mN m⁻¹, leading the shells to form a more accurate representation of the initial clusters. The new cluster is then re-evolved with a lower shell/water tension into the same type of symmetric cluster achieved when low shell/water surface tensions are applied *ab initio*.

ASSOCIATED CONTENT

S Supporting Information

The Supporting Information is available free of charge on the ACS Publications website at DOI: 10.1021/acsnano.8b00521.

Experimental details, materials and measurements, synthetic limitations, supplementary microscopy images, simulation protocol, and Surface Evolver script (PDF)

AUTHOR INFORMATION

Corresponding Author

*E-mail: s.sacanna@nyu.edu.

ORCID ®

Stefano Sacanna: 0000-0002-8399-3524

Notes

The authors declare no competing financial interest.

ACKNOWLEDGMENTS

This work was supported by the NSF CAREER award DMR-1653465. The Zeiss Merlin FESEM was acquired through the support of the NSF under award number DMR-0923251.

REFERENCES

- (1) Maldovan, M. Sound and Heat Revolutions in Phononics. *Nature* **2013**, *503*, 209.
- (2) Maldovan, M.; Thomas, E. L. Simultaneous Localization of Photons and Phonons in Two-Dimensional Periodic Structures. *Appl. Phys. Lett.* **2006**, *88*, 251907.
- (3) Saranathan, V.; Osuji, C. O.; Mochrie, S. G.; Noh, H.; Narayanan, S.; Sandy, A.; Dufresne, E. R.; Prum, R. O. Structure, Function, and Self-Assembly of Single Network Gyroid (I4132) Ghotonic Crystals in Butterfly Wing Scales. *Proc. Natl. Acad. Sci. U. S. A.* **2010**, *107*, 11676—11681
- (4) Veselago, V.; Narimanov, E. The Left Hand of Brightness: Past, Present and Future of Negative Index Materials. *Nat. Mater.* **2006**, *5*, 759.
- (5) Yablonovitch, E. Photonic Band-Gap Structures. J. Opt. Soc. Am. B 1993, 10, 283–295.
- (6) Ho, K.; Chan, C. T.; Soukoulis, C. M. Existence of a Photonic Gap in Periodic Dielectric Structures. *Phys. Rev. Lett.* **1990**, *65*, 3152.
- (7) Yablonovitch, E. Photonic Crystals: Semiconductors of Light. *Sci. Am.* **2001**, 285, 47.
- (8) Nielson, R.; Kaehr, B.; Shear, J. B. Microreplication and Design of Biological Architectures Using Dynamic-Mask Multiphoton Lithography. *Small* **2009**, *5*, 120–125.
- (9) Haske, W.; Chen, V. W.; Hales, J. M.; Dong, W.; Barlow, S.; Marder, S. R.; Perry, J. W. 65 nm Feature Sizes Using Visible Wavelength 3-D Multiphoton Lithography. *Opt. Express* **2007**, *15*, 3426–3436.
- (10) Juodkazis, S.; Mizeikis, V.; Seet, K. K.; Miwa, M.; Misawa, H. Two-photon Lithography of Nanorods in SU-8 Photoresist. *Nanotechnology* **2005**, *16*, 846.
- (11) Kawata, S.; Sun, H.-B.; Tanaka, T.; Takada, K. Finer Features for Functional Microdevices. *Nature* **2001**, *412*, 697–698.
- (12) Glotzer, S.; Solomon, M.; Kotov, N. A. Self-Assembly: From Nanoscale to Microscale Colloids. *AIChE J.* **2004**, *50*, 2978–2985.
- (13) Damasceno, P. F.; Engel, M.; Glotzer, S. C. Predictive Self-Assembly of Polyhedra into Complex Structures. *Science* **2012**, 337, 453–457
- (14) Hynninen, A.-P.; Thijssen, J. H.; Vermolen, E. C.; Dijkstra, M.; Van Blaaderen, A. Self-Assembly Route for Photonic Crystals with a Bandgap in the Visible Region. *Nat. Mater.* **2007**, *6*, 202–205.
- (15) Cademartiri, L.; Bishop, K. J.; Snyder, P. W.; Ozin, G. A. Using Shape for Self-Assembly. *Philos. Trans. R. Soc., A* **2012**, 370, 2824–2847
- (16) Halverson, J. D.; Tkachenko, A. V. DNA-Programmed Mesoscopic Architecture. *Phys. Rev. E* **2013**, *87*, 062310.
- (17) Demirors, A. F.; van Blaaderen, A.; Imhof, A. A General Method to Coat Colloidal Particles with Titania. *Langmuir* **2010**, *26*, 9297–9303.
- (18) Rossi, L.; Sacanna, S.; Irvine, W. T.; Chaikin, P. M.; Pine, D. J.; Philipse, A. P. Cubic Crystals from Cubic Colloids. *Soft Matter* **2011**, *7*, 4139–4142.
- (19) Castillo, S. I.; Krans, N. A.; Pompe, C. L.; den Otter, J. A.; Thies-Weesie, D. M.; Philipse, A. P. Synthesis Method for Crystalline Hollow Titania Micron-Cubes. *Colloids Surf., A* **2016**, *504*, 228–233.
- (20) Youssef, M.; Hueckel, T.; Yi, G.-R.; Sacanna, S. Shape-Shifting Colloids *via* Stimulated Dewetting. *Nat. Commun.* **2016**, *7*, 1221610.1038/ncomms12216.
- (21) Graf, C.; van Blaaderen, A. Metallodielectric colloidal core-shell particles for photonic applications. *Langmuir* **2002**, *18*, 524–534.
- (22) Liu, Y.; Edmond, K. V.; Curran, A.; Bryant, C.; Peng, B.; Aarts, D. G.; Sacanna, S.; Dullens, R. Core-Shell Particles for Simultaneous 3D Imaging and Optical Tweezing in Dense Colloidal Materials. *Adv. Mater.* **2016**, 28, 8001–8006.

(23) Gu, S.; Onishi, J.; Mine, E.; Kobayashi, Y.; Konno, M. Preparation of Multilayered Gold-Silica-Polystyrene Core-Shell Particles by Seeded Polymerization. *J. Colloid Interface Sci.* **2004**, 279, 284–287.

- (24) Sacanna, S.; Korpics, M.; Rodriguez, K.; Colón-Meléndez, L.; Kim, S.-H.; Pine, D. J.; Yi, G.-R. Shaping Colloids for Self-Assembly. *Nat. Commun.* **2013**, *4*, 1688.
- (25) Désert, A.; Chaduc, I.; Fouilloux, S.; Taveau, J.-C.; Lambert, O.; Lansalot, M.; Bourgeat-Lami, E.; Thill, A.; Spalla, O.; Ravaine, S.; Duguet, E. High-Yield Preparation of Polystyrene/Silica Clusters of Controlled Morphology. *Polym. Chem.* **2012**, *3*, 1130–1132.
- (26) Wang, Y.; Wang, Y.; Breed, D. R.; Manoharan, V. N.; Feng, L.; Hollingsworth, A. D.; Weck, M.; Pine, D. J. Colloids with Valence and Specific Directional Bonding. *Nature* **2012**, *491*, 51–55.
- (27) Wang, Y.; Hollingsworth, A. D.; Yang, S. K.; Patel, S.; Pine, D. J.; Weck, M. Patchy Particle Self-Assembly *via* Metal Coordination. *J. Am. Chem. Soc.* **2013**, *135*, 14064–14067.
- (28) Désert, A.; Hubert, C.; Fu, Z.; Moulet, L.; Majimel, J.; Barboteau, P.; Thill, A.; Lansalot, M.; Bourgeat-Lami, E.; Duguet, E.; Ravaine, S. Synthesis and Site-Specific Functionalization of Tetravalent, Hexavalent, and Dodecavalent Silica Particles. *Angew. Chem., Int. Ed.* **2013**, *52*, 11068–11072.
- (29) Hubert, C.; Chomette, C.; Désert, A.; Sun, M.; Treguer-Delapierre, M.; Mornet, S.; Perro, A.; Duguet, E.; Ravaine, S. Synthesis of Multivalent Silica Nanoparticles Combining both Enthalpic and Entropic Patchiness. *Faraday Discuss.* **2015**, *181*, 139–146.
- (30) Wang, H.; Li, B.; Yodh, A. G.; Zhang, Z. Stimuli-Responsive Shape Switching of Polymer Colloids by Temperature-Sensitive Absorption of Solvent. *Angew. Chem.* **2016**, *128*, 10106–10109.
- (31) Vutukuri, H. R.; Imhof, A.; Van Blaaderen, A. Fabrication of Polyhedral Particles from Spherical Colloids and Their Self-Assembly into Rotator Phases. *Angew. Chem., Int. Ed.* **2014**, *53*, 13830–13834.
- (32) Gong, Z.; Hueckel, T.; Yi, G.-R.; Sacanna, S. Patchy Particles Made by Colloidal Fusion. *Nature* **2017**, *550*, 234.
- (33) Hilgenfeldt, S.; Kraynik, A.; Reinelt, D.; Sullivan, J. The Structure of Foam Cells: Isotropic Plateau Polyhedra. *Europhys. Lett.* **2004**, *67*, 484.
- (34) Schade, N. B.; Holmes-Cerfon, M. C.; Chen, E. R.; Aronzon, D.; Collins, J. W.; Fan, J. A.; Capasso, F.; Manoharan, V. N. Tetrahedral Colloidal Clusters from Random Parking of Bidisperse Spheres. *Phys. Rev. Lett.* **2013**, *110*, 148303.
- (35) Ducrot, É.; He, M.; Yi, G.-R.; Pine, D. J. Colloidal Alloys with Preassembled Clusters and Spheres. *Nat. Mater.* **2017**, *16*, 65210.1038/nmat4869.
- (36) Wang, Y.; Wang, Y.; Zheng, X.; Yi, G.-R.; Sacanna, S.; Pine, D. J.; Weck, M. Three-Dimensional Lock and Key Colloids. *J. Am. Chem. Soc.* **2014**, *136*, 6866–6869.
- (37) Zheng, X.; Wang, Y.; Wang, Y.; Pine, D. J.; Weck, M. Thermal Regulation of Colloidal Materials Architecture through Orthogonal Functionalizable Patchy Particles. *Chem. Mater.* **2016**, 28, 3984–3989.
- (38) Brakke, K. A. The Surface Evolver. Exp. Math. 2012, 1, 141–165.
- (39) Chen, Q.; Bae, S. C.; Granick, S. Directed Self-Assembly of a Colloidal Kagome Lattice. *Nature* **2011**, *469*, 381–384.
- (40) Chen, Q.; Yan, J.; Zhang, J.; Bae, S. C.; Granick, S. Janus and Multiblock Colloidal Particles. *Langmuir* **2012**, *28*, 13555–13561.
- (41) Wang, Y.; Wang, Y.; Zheng, X.; Ducrot, E.; Lee, M.-G.; Yi, G.-R.; Weck, M.; Pine, D. J. Synthetic Strategies Toward DNA-Coated Colloids that Crystallize. *J. Am. Chem. Soc.* **2015**, *137*, 10760–10766.
- (42) Sugimoto, T.; Khan, M. M.; Muramatsu, A. Preparation of Monodisperse Peanut-Type α -Fe2O3 Particles from Condensed Ferric Hydroxide Gel. *Colloids Surf.*, A 1993, 70, 167–169.
- (43) Stöber, W.; Fink, A.; Bohn, E. Controlled Growth of Monodisperse Silica Spheres in the Micron Size Range. *J. Colloid Interface Sci.* **1968**, *26*, 62–69.
- (44) Sacanna, S.; Rossi, L.; Kuipers, B.; Philipse, A. Fluorescent Monodisperse Silica Ellipsoids for Optical Rotational Diffusion Studies. *Langmuir* **2006**, *22*, 1822–1827.

(45) Westcott, S. L.; Oldenburg, S. J.; Lee, T. R.; Halas, N. J. Formation and Adsorption of Clusters of Gold Nanoparticles onto Functionalized Silica Nanoparticle Surfaces. *Langmuir* **1998**, *14*, 5396–5401.